


 Cite this: *RSC Adv.*, 2025, 15, 38743

# Iron-catalyzed divergent synthesis of coumarin fused N-heterocycles *via* 6 $\pi$ -electrocyclization and isoxazole ring-opening

 Sakshi Singh, Manthri Atchuta Rao, Samir Kumar Mondal and Shantanu Pal \*

We have developed a facile, iron-catalyzed one-pot strategy for the regioselective synthesis of chromeno [4,3-*b*]quinolin-6-one derivatives. This transformation proceeds *via* a three-component tandem annulation involving 4-hydroxycoumarin, aldehydes, and anilines, through a one-pot imine formation followed by a 6 $\pi$ -electrocyclization under acidic conditions. Furthermore, we extended this methodology to a three-component annulation of 4-hydroxycoumarin with ammonium acetate and isoxazole derivatives, proceeding *via* iron-catalyzed Michael-type addition of isoxazoles, followed by ring opening and subsequent cyclization towards synthesis of chromeno[4,3-*b*]pyridine. The photophysical properties of the resulting fused heterocycles showed moderate to good fluorescence quantum yields.

 Received 15th September 2025  
 Accepted 9th October 2025

DOI: 10.1039/d5ra06995e

[rsc.li/rsc-advances](https://rsc.li/rsc-advances)

## Introduction

Coumarin is a vital and widely occurring structural scaffold, present in many natural products, bioactive compounds and renowned for its prominent role in sensor devices due to its unique electronic properties.<sup>1</sup> Notably, coumarin-fused polycyclic compounds represent a distinctive and highly valuable class of fused heterocyclic hybrids, frequently encountered in the core structures of numerous pharmacologically active compounds and natural products.<sup>2</sup> These frameworks are integral to various bioactive natural products like schumanniphytine and pheofungin A as illustrated in Fig. 1.<sup>3</sup> Building on the significance of chromeno-quinoline scaffolds, an emerging strategy in modern drug design involves the fusion of two distinct pharmacophores into a single molecular framework known as pharmacophore hybridization.<sup>4</sup> In addition to coumarin-derived frameworks, fused heterocyclic systems incorporating 1,4-dihydropyridines (1,4-DHPs) are of significant interest due to the well-established pharmacological relevance of the DHP core such as calcium channel modulators, antihypertensive, antimicrobial, and antioxidant properties.<sup>5</sup> In general, conventional methods involve pre-functionalization of the starting materials and require multi step transformations as presented in Scheme 1.<sup>6</sup> In this context, the development of efficient synthetic methods represent a major challenge in accessing such complex hybrid scaffolds. Multicomponent reactions (MCRs) have emerged as efficient approach for the synthesis of such complex fused molecules by enabling the simultaneous formation of multiple bonds from readily available starting materials in a one-pot, atom-economical process.<sup>7</sup>

Over the past few decades, several methods have been developed for the three-component synthesis of chromeno[4,3-*b*]quinolin-6-one derivatives.<sup>8</sup> However, literature reports indicate that the use of aromatic amines as 1,3-binucleophiles in MCRs remains relatively less explored and is predominantly limited to reactions involving aromatic aldehydes.<sup>9</sup> To address these limitations, we initially hypothesized that the combination of 4-hydroxycoumarin, aldehyde, and aromatic amine could yield either product **4** or **4'**, as outlined in Scheme 1, depending on the reaction pathway through 6 $\pi$ -electrocyclization or Skraup–Doebner–von Miller reaction.<sup>10</sup> To overcome the selectivity challenge, we employed an iron-catalyzed approach, as iron salts are inexpensive, stable, low in toxicity, and environmentally benign make them an ideal alternative to noble metals catalysis while also utilizing air as a green oxidant, further enhancing the sustainability and practicality of the system.<sup>11</sup> Herein, we developed an efficient, selective synthesis

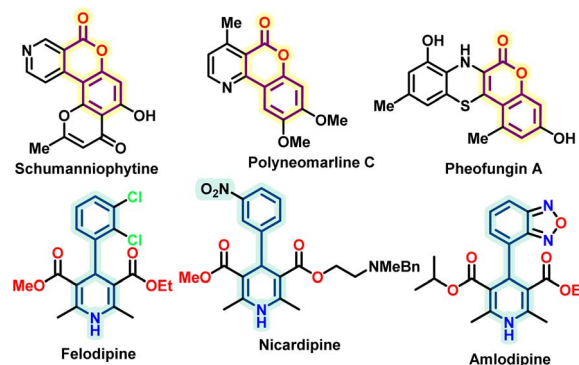
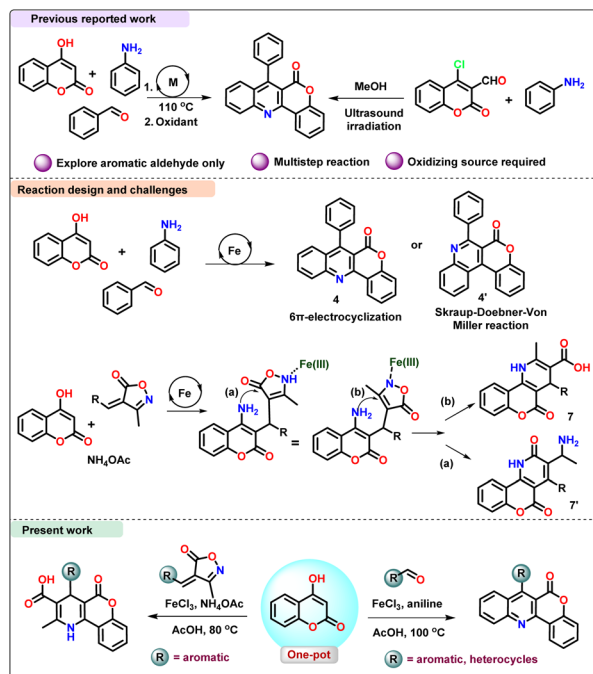


Fig. 1 Representative example of chromeno-quinoline and 1,4 DHP based biologically active compounds.

School of Basic Sciences (Chemistry), Indian Institute of Technology Bhubaneswar, Argul, Khordha-752050, Odisha, India. E-mail: [spal@iitbbs.ac.in](mailto:spal@iitbbs.ac.in); [ss122@iitbbs.ac.in](mailto:ss122@iitbbs.ac.in)





Scheme 1 Previous work, reaction design and challenges and present work.

of chromeno[4,3-*b*]quinolin-6-one *via* an iron-catalyzed three-component tandem annulation involving 4-hydroxycoumarin, aldehyde, and aniline. The transformation proceeds through a one-pot imine formation followed by a 6 $\pi$ -electrocyclization under acidic conditions.

In addition, isoxazoles have gained prominence as versatile precursors for constructing diverse heterocycles.<sup>12</sup> This reactive feature has been harnessed in various transformations, including hydrolysis reaction towards synthesis of heterocycles.<sup>13</sup> The controlled multicomponent exploitation of reactive isoxazole intermediates offers a powerful route to molecular diversification and drug-like scaffolds; however, iron-catalyzed strategies for their transformation remain unexplored, with no prior reports on the synthesis of coumarin-fused heterocycles.

In this context, we design our approach involving a three-component annulation of 4-hydroxycoumarin, isoxazole derivative and ammonium acetate. We hypothesized that the reaction proceeds *via* a 4-aminocoumarin intermediate, which undergoes path (a) or path (b) nucleophilic attack on the isoxazole derivative, afforded either product 7 or 7', depending on the reaction pathway, as illustrated in Scheme 1. Here we present Fe-catalyzed Michael type nucleophilic attack on the isoxazole derivative, followed by cyclization towards selective synthesis of coumarin-fused 1,4-dihydropyridine 7 frameworks enabling the in a one-pot approach.

## Results and discussion

To optimize the reaction conditions for the synthesis of compound **4a**, a series of experiments were conducted by

varying catalysts, solvents, additives, and temperature, as summarized in Table 1, beginning with the reaction of aniline **1** and benzaldehyde **2**, followed by the addition of 4-hydroxycoumarin **3** in acetic acid at room temperature. However, the starting materials still remained at room temperature (Table 1, entry 1). Furthermore, increasing the reaction temperature from 50 °C to 100 °C resulted in only 30% product formation (Table 1, entry 2). Based on our previous research interest in iron-catalyzed transformations and the potential of iron(III) salts to act as Lewis acid to accelerate the three component reaction. Upon adding a catalytic amount of FeCl<sub>3</sub> to the reaction mixture, we observed a significant increase in product yield, reaching up to 87% (Table 1, entry 3). To further optimize the reaction, we screened various catalysts such as FeCl<sub>2</sub>, Fe-powder, ZnCl<sub>2</sub>, CuI and Cu(OTf)<sub>2</sub> and found FeCl<sub>3</sub> to be the most effective for promoting this three-component annulation (Table 1, entries 3–8). A comprehensive solvent screening was carried out using a range of solvents, including DMSO, toluene, DCE, isopropanol, and water; however, none of these supported the formation of the desired product **4a**. Other solvents such as trifluoroacetic acid (TFA), 1,4-dioxane, DMF, and acetonitrile afforded only moderate to low yields. These observations clearly indicate that acetic acid (AcOH) was the most suitable solvent for promoting the annulation reaction and achieving optimal product yield (Table 1, entries 9–17). It was observed that the

Table 1 Selected optimization studies<sup>a</sup>

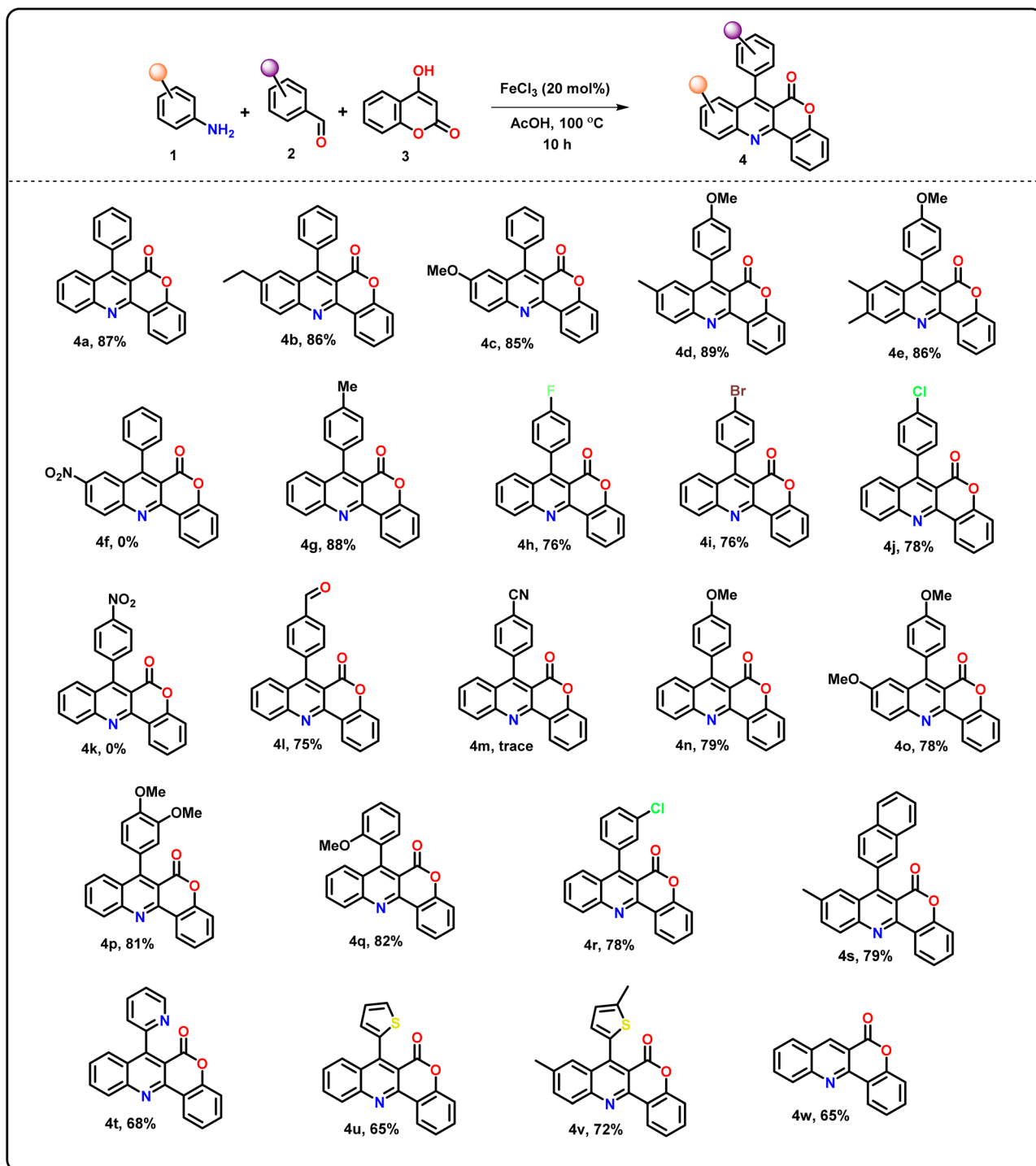
Entry	Catalyst	Solvent	Temperature	4a yield <sup>b</sup>
1	—	AcOH	rt	n.d.
2	—	AcOH	100 °C	30%
3	FeCl <sub>3</sub>	AcOH	100 °C	87%
4	FeCl <sub>2</sub>	AcOH	100 °C	10%
5	Fe-powder	AcOH	100 °C	Trace
6	ZnCl <sub>2</sub>	AcOH	100 °C	20%
7	CuI	AcOH	100 °C	n.d.
8	Cu(OTf) <sub>2</sub>	AcOH	100 °C	n.d.
9	FeCl <sub>3</sub>	TFA	100 °C	Trace
10	FeCl <sub>3</sub>	1,4-Dioxane	100 °C	20%
11	FeCl <sub>3</sub>	DMF	100 °C	10%
12	FeCl <sub>3</sub>	DMSO	100 °C	n.d.
13	FeCl <sub>3</sub>	Toluene	100 °C	n.d.
14	FeCl <sub>3</sub>	CH <sub>3</sub> CN	100 °C	20%
15	FeCl <sub>3</sub>	DCE	100 °C	n.d.
16	FeCl <sub>3</sub>	Isopropanol	100 °C	n.d.
17	FeCl <sub>3</sub>	H <sub>2</sub> O	100 °C	n.d.
18	FeCl <sub>3</sub>	—	100 °C	n.d.
19 <sup>c</sup>	FeCl <sub>3</sub>	AcOH	100 °C	10%
20 <sup>d</sup>	FeCl <sub>3</sub>	AcOH	100 °C	70%
21	—	HCl	100 °C	10%

<sup>a</sup> Reactions condition **1a** (0.5 mmol), **2a** (0.5 mmol), **3a** (0.5 mmol) and catalyst (20 mol%) in 2 ml of solvent for 10 h. <sup>b</sup> Isolated yield. <sup>c</sup> Under N<sub>2</sub> atmosphere. <sup>d</sup> Catalyst (10 mol%).



coupling product did not form in the absence of AcOH (Table 1, entry 18). Additionally, conducting the reaction under a nitrogen atmosphere resulted in less than 10% product yield, confirming that aerobic conditions are essential for the reaction to proceed efficiently (Table 1, entry 19). Reducing the catalyst loading from 20 mol% to 10 mol% led to a decrease in the product yield (Table 1, entry 20).

On the other hand, when the reaction was carried out using a Brønsted acid (HCl), only 10% of the cyclized product was obtained (Table 1, entry 21). Based on the above observations and optimization of the catalyst loading, it was found that 20 mol% FeCl<sub>3</sub> in AcOH solvent was the best condition for cyclization. With the optimized reaction conditions in hand, we next explored the substrate scope of the multicomponent annulation for the synthesis of chromeno[4,3-*b*]quinolin-6-one



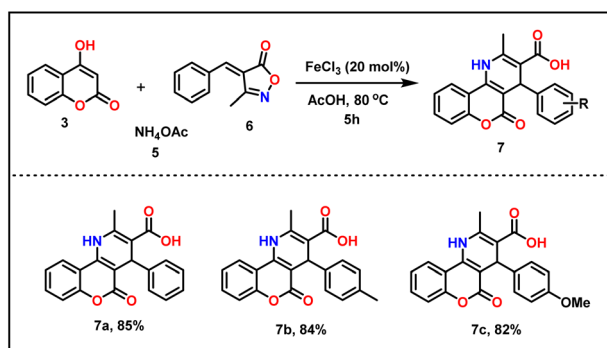
Scheme 2 Substrate scope of chromeno[4,3-*b*]quinolin-6-one derivatives.



derivatives **4**. In the initial part, a variety of aniline derivatives bearing substituents such as methyl, ethyl, methoxy, dimethyl, and nitro were evaluated. The reaction exhibited good tolerance toward electron-rich anilines for synthesis of compound (**4a–e**, **4o**) with 78–87% yields, while electron-deficient substituents like nitro failed to undergo the desired transformation **4f**. Similarly, a range of aromatic aldehydes substituted with methyl, methoxy, fluoro, bromo, chloro, *o*-methoxy, *m*-chloro, and CHO groups participated efficiently in the annulation and synthesized the respective products (**4g–j**, **l** and **n–r**) with 70–88% yield, except for electron withdrawing substituted aldehydes such as nitro, cyano attach group were unreactive to deliver the product (**4k**, **m**). Notably, the protocol also accommodated heteroaromatic aldehydes such as 2-thiophene, naphthalene, 5-methyl-2-thiophene, and 2-pyridine, affording the corresponding chromeno[4,3-*b*]quinolin-6-one products (**4s–v**) with 79–65% yields. Furthermore, formaldehyde was well-tolerated, delivering the desired product **4w** in comparable yields (Scheme 2).

Under the optimized reaction conditions, we further explored the substrate scope for the synthesis of 2-methyl-5-oxo-4-phenyl-1,5-dihydro-4*H*-chromeno[4,3-*b*]pyridine-3-carboxylic acid derivatives **7**, as illustrated in Scheme 3. This transformation represents another three-component coupling reaction, wherein 4-hydroxycoumarin was first treated with ammonium acetate, followed by the addition of (*E*)-4-benzylidene-3-methylisoxazol-5(*4H*)-one **6** (detail synthesis procedure in SI) in acetic acid under standard condition delivered 75% yield. After temperature screening, we found that the reaction also proceeded efficiently at 80 °C, affording the annulated product in 85% yield.

After the successful synthesis of compound **7**, we further investigated the substrate scope of (*E*)-4-benzylidene-3-methylisoxazol-5(*4H*)-one **6** by varying the substituents on the phenyl ring. Substrates bearing electron-donating groups such as methyl and methoxy were well tolerated under the standard reaction conditions, affording the desired three-component annulated products in good yields. In contrast, substrates containing electron-withdrawing groups failed to produce the target products, indicating a limitation of the reaction with electron-deficient aryl systems. While previous studies have

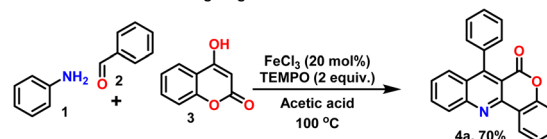


Scheme 3 Substrate scope of 2-methyl-5-oxo-4-phenyl-1,5-dihydro-4*H*-chromeno[4,3-*b*]pyridine-3-carboxylic acid.

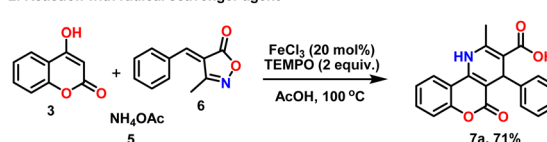
primarily focused on Fe-mediated cleavage of the isoxazole ring under acidic conditions, often leading to one-pot intramolecular transformations such as cyclizations or heterocycle to heterocycle rearrangements. We demonstrate the novel example of ring-cleaved intermediate generated under FeCl<sub>3</sub> catalysis mild acidic condition efficiently harnessed in a three-component annulation reaction. This transformation not only proceeds smoothly under mild conditions but also enables the rapid assembly of structurally complex and pharmaceutically relevant heterocycles.

In order to understand the mechanistic pathway and validate the role of individual components in the FeCl<sub>3</sub>-catalyzed three-component annulation reaction, some control experiments were performed. To examine whether the iron-catalyzed annulation proceeds through a radical pathway, we carried out radical-trapping experiments using TEMPO as a scavenger. The reactions were conducted in the presence of TEMPO under the standard conditions. In both cases, the desired products **4a** and **7a** were obtained in comparable yields to the control reactions, indicating that the reaction pathway does not involve radical intermediates. Additional mechanistic insights were gained by examining the effect of the sequence of component addition. It was observed that simultaneous addition of all three components aniline **1**, benzaldehyde **2**, and 4-hydroxycoumarin **3** led to a decrease in product yield. In contrast, a stepwise approach preforming the imine intermediate by reacting compound **1** and **2** at room temperature, followed by the addition of 4-

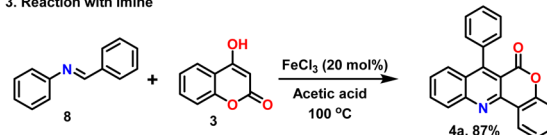
#### 1. Reaction with radical scavenger agent



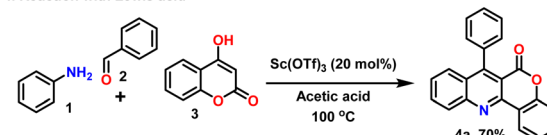
#### 2. Reaction with radical scavenger agent



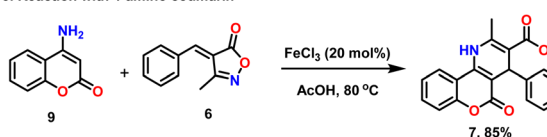
#### 3. Reaction with imine



#### 4. Reaction with Lewis acid



#### 5. Reaction with 4-amino coumarin



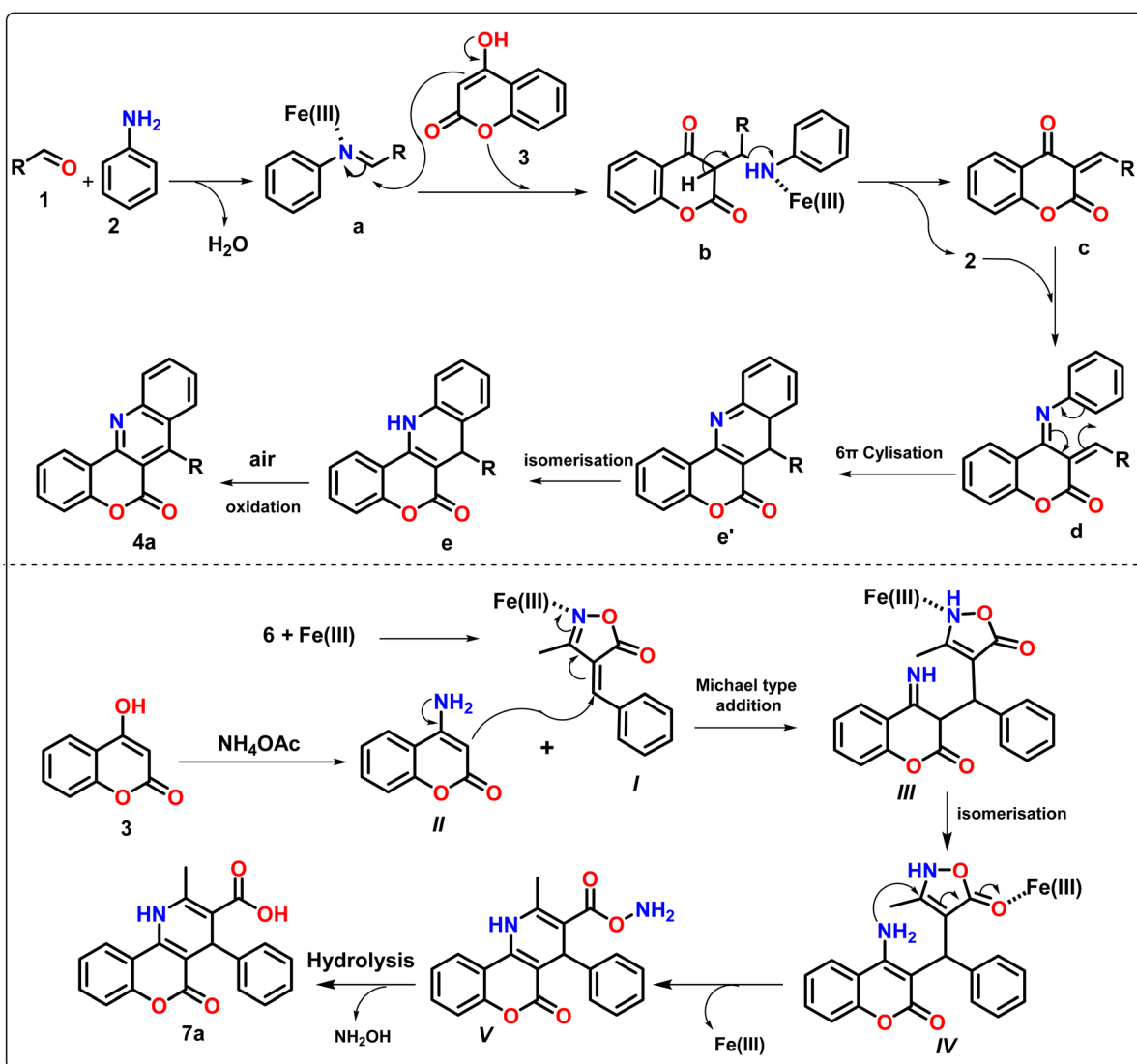
Scheme 4 Control experiments.



hydroxycoumarin in acetic acid resulted in a significantly improved yield. This observation prompted the independent synthesis and reaction of the imine intermediate with 4-hydroxycoumarin, which successfully delivered product **4a** in high yield, confirming the imine as a key intermediate in the annulation pathway. To assess the role of  $\text{FeCl}_3$ , the reaction was also conducted using  $\text{Sc}(\text{OTf})_3$  as an alternative Lewis acid. The formation of product **4a** in comparable yield indicated that  $\text{FeCl}_3$  primarily functions as a Lewis acid to promote the transformation. To further understand the reaction pathway, the reaction between 4-amino coumarin **9** and isoxazole derivative **6** were carried out under optimized conditions, affording compound **7** in 86% yield. This result supports the initial formation of 4-amino coumarin, followed by its subsequent reaction (Scheme 4).

Based on control experiments and supporting literature, we have proposed a plausible reaction mechanism. Specifically, we describe two distinct three-component annulation pathways

involving 4-hydroxycoumarin, each following a different activation and cyclization mechanism (Scheme 5). In the first mechanistic pathway, the reaction begins with the *in situ* formation of imine intermediate **a** from aniline and benzaldehyde, which undergoes nucleophilic attack by 4-hydroxycoumarin at the imine carbon facilitated by  $\text{FeCl}_3$  under acidic conditions. In the subsequent step, elimination of aniline leads to the formation of a stable intermediate **c**, which further undergoes a 1, 2-addition of aniline followed by  $6\pi$ -electrocyclization. Resulting intermediate **e** undergoes oxidative aromatization to furnish the chromeno[4,3-*b*]quinolin-6-one scaffold **4**. On the other hand, the second annulation pathway begins with the reaction of 4-hydroxycoumarin and ammonium acetate, resulting in the formation of 4-aminocoumarin intermediate **II**. Subsequently, treatment of the isoxazole derivative **6** with  $\text{FeCl}_3$  leads to the formation of intermediate **I**, which undergoes Michael type nucleophilic attack by 4-aminocoumarin at the electrophilic benzyldiene carbon, resulting in

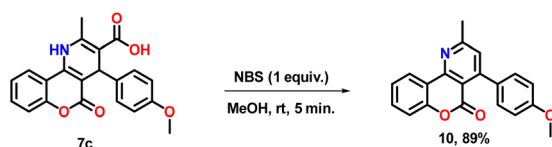


Scheme 5 Plausible mechanism.



the formation of intermediate **III**. Following this isomerisation and nucleophilic attack of  $\text{NH}_2^-$  on the  $\beta$ -carbon of carbonyl yields to intermediate **V** and subsequent hydrolysis leading to the formation of the desired product **7**.

After successfully establishing the iron-catalyzed tandem cyclization, we evaluated the practicality of the methodology by scaling up the reaction to the gram scale, which afforded compound **7a** in 75% yield. Furthermore, compound **7c** underwent efficient decarboxylation and aromatization upon treatment with *N*-bromosuccinimide (NBS) in methanol at room temperature. The reaction was completed within 5 minutes, yielding compound **10** in 89% yield (Scheme 6).



Scheme 6 Synthesis of 4-(4-methoxyphenyl)-2-methyl-5H-chromeno[4,3-*b*]pyridin-5-one.

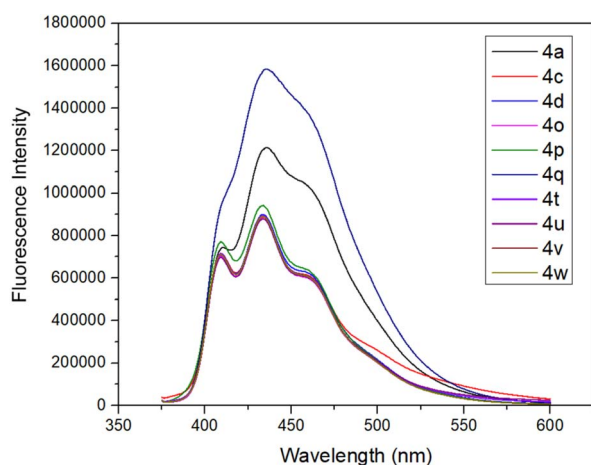


Fig. 2 Emission spectra of **4a**, **4c**, **4d**, **4o**, **4p**, **4q**, **4t**, **4u**, **4v** and **4w** in  $\text{CHCl}_3$  ( $5 \times 10^{-6} \text{ mol L}^{-1}$ ).

Table 2 Photophysical properties

Compound	$\lambda_{\text{abs max}}^a$ (nm)	$\lambda_{\text{em max}}^b$ (nm)	$\log \epsilon$	$\Phi_{\text{F}}^c$
<b>4a</b>	359	436	3.65	0.49
<b>4c</b>	381	434	3.54	0.39
<b>4d</b>	368	433	3.81	0.20
<b>4o</b>	382	433	3.65	0.28
<b>4p</b>	364	434	3.84	0.19
<b>4q</b>	358	436	3.60	0.83
<b>4t</b>	375	433	3.69	0.26
<b>4u</b>	365	434	3.54	0.36
<b>4v</b>	374	433	3.67	0.27
<b>4w</b>	349	433	3.17	0.86

<sup>a</sup> Absorption maxima in  $\text{CHCl}_3$  ( $5 \times 10^{-6} \text{ mol L}^{-1}$ ). <sup>b</sup> Emission maxima in  $\text{CHCl}_3$  ( $5 \times 10^{-6} \text{ mol L}^{-1}$ ). <sup>c</sup> Fluorescence quantum yield, determined by quinine sulfate ( $\Phi_{\text{F}} = 0.546$  in  $\text{H}_2\text{SO}_4$ ).

In addition, the photophysical properties of the selectively synthesized coupling products (**4a**, **4c**, **4d**, **4o**, **4p**, **4q**, **4t**, **4u**, **4v**, and **4w**) were investigated through fluorescence emission and UV-visible spectroscopy in  $\text{CHCl}_3$  at a concentration of  $5 \times 10^{-6} \text{ M}$  (Fig. 2). The UV-visible spectra of these selected derivatives display absorption bands ranging from 250 to 400 nm, typically comprising two to three distinct peaks. These peaks are attributed to different electronic transitions, such as  $n \rightarrow \pi^*$  and  $\pi \rightarrow \pi^*$  transitions. The emission maxima ( $\lambda_{\text{em(max)}}$ ) for these derivatives are observed in the range of 430–440 nm. Notably, these compounds exhibit strong fluorescence with high quantum yields ( $\Phi_{\text{F}}$ ) reaching up to 0.86, indicating excellent photophysical property (Table 2).

## Conclusion

In conclusion, we have developed an efficient and straightforward iron(III)-catalyzed one-pot three-component annulation strategy for the selective synthesis of two distinct coumarin-fused heterocycles: 7-phenyl-6H-chromeno[4,3-*b*]quinolin-6-one and 2,4-dimethyl-5-oxo-1,5-dihydro-4H-chromeno[4,3-*b*]pyridine-3-carboxylic acid. This work highlights two divergent multicomponent reaction pathways using 4-hydroxycoumarin as the common starting material. The first pathway proceeds *via* a imine formation followed by  $6\pi$ -electrocyclization then aromatization, leading to chromeno[4,3-*b*]quinolin-6-one derivatives. The second involves nucleophilic attack and subsequent ring-opening of isoxazoles, affording chromeno[4,3-*b*]pyridine-3-carboxylic acid analogues. Both methods are atom-economical, operationally simple, and provide access to structurally diverse coumarin-fused heterocycles. Additionally, photophysical studies of the synthesized compounds revealed moderate to good fluorescence quantum yields, indicating their potential utility as fluorescent sensors. The construction of diverse hybrid drug-like scaffolds highlights their broad potential for applications in both medicinal and materials chemistry.

## Conflicts of interest

There are no conflicts of interest.

## Data availability

The data supporting this article have been included as part of the supplementary information (SI). Supplementary information is available. See DOI: <https://doi.org/10.1039/d5ra06995e>.

## Acknowledgements

This research work is financially supported by the Ministry of Earth Science (MoES) (sanction letter number: MoES/PAMC/DOM/181/2023(E14616)) is greatly acknowledged.



## Notes and references

- 1 (a) I. A. Khan, M. V. Kulkarni, M. Gopal, M. S. Shahabuddin and C. M. Sun, *Bioorg. Med. Chem. Lett.*, 2005, **15**, 3584–3587; (b) J. Chen, W. Liu, J. Ma, H. Xu, J. Wu, X. Tang, Z. Fan and P. Wang, *J. Org. Chem.*, 2012, **77**, 3475–3482; (c) K. N. Venugopala, V. Rashmi and B. Odhav, *BioMed Res. Int.*, 2013, **1**, 963248; (d) S. Tandon and R. P. Rastogi, *J. Sci. Ind. Res.*, 1979, **38**, 428–441; (e) K. Szwaczko, *Curr. Org. Chem.*, 2023, **27**, 1329–1335.
- 2 (a) A. T. Vu, A. N. Campbell, H. A. Harris, R. J. Unwalla, E. S. Manas and R. E. Mewshaw, *Bioorg. Med. Chem. Lett.*, 2007, **17**, 4053–4056; (b) F. Salehian, H. Nadri, L. Jalili-Baleh, L. Youseftabar-Miri, S. N. A. Bukhari, A. Foroumadi, T. T. Küçükkinç, M. Sharifzadeh and M. Khoobi, *Eur. J. Med. Chem.*, 2021, **212**, 113034; (c) F. G. Medina, J. G. Marrero, M. M. Alonso, M. C. Gonzalez, I. C. Guerrero, A. G. T. Garcia and S. O. Robles, *Nat. Prod. Rep.*, 2015, **32**, 1472–1507.
- 3 (a) K. Scherlach, H. W. Nutzmann, V. Schroeckh, H. M. Dahse, A. A. Brakhage and C. Hertweck, *Angew. Chem., Int. Ed.*, 2011, **50**, 9843–9847; (b) M. D. Markey, Y. Fu and T. R. Kelly, *Org. Lett.*, 2007, **9**, 3255–3257.
- 4 S. Choudhary, P. K. Singh, H. Verma, H. Singh and O. Silakari, *Eur. J. Med. Chem.*, 2018, **151**, 62–97.
- 5 (a) A. Parthiban and P. Makam, *RSC Adv.*, 2022, **12**, 29253–29290; (b) T. Yamamoto, S. Niwa, M. Tokumasu, T. Onishi, S. Ohno, M. Hagihara, H. Koganei, S. Fujita, T. Takeda, Y. Saitou, S. Iwayama, A. Takahara, S. Iwata and M. Shoji, *Bioorg. Med. Chem. Lett.*, 2012, **22**, 3639–3642; (c) A. Velena, N. Zarkovic, K. G. Troselj, E. Bisenieks, A. Krauze, J. Poikans and G. Duburs, *Oxid. Med. Cell. Longevity*, 2016, **1**, 1892412; (d) L. Suresh, P. S. V. Kumar, P. Onkar, L. Srinivas, Y. Pydisetty and G. V. P. Chandramouli, *Res. Chem. Intermed.*, 2017, **43**, 5433–5451; (e) H. E. Sellitepe, İ. S. Doğan, G. Eroğlu, B. Barut and A. Özel, *J. Res. Pharm.*, 2019, **23**, 608–616; (f) H. S. Sohal, *Mater. Today: Proc.*, 2022, **48**, 1163–1170; (g) A. F. S. Lago, D. F. C. Benedicto, L. Silva and S. S. Thomasi, *Curr. Org. Chem.*, 2023, **27**, 1567–1610.
- 6 (a) Z. Chen, J. Gu and W. Su, *J. Chem. Res.*, 2013, **44**, 327–330; (b) P. Patra, *Org. Prep. Proced. Int.*, 2021, **53**, 184–189; (c) J. V. Prasad, J. S. Reddy, N. R. kumar, K. A. Solomon and G. Gopikrishna, *J. Chem. Sci.*, 2011, **123**, 673–679; (d) D. Garella, A. Barge, D. Upadhyaya, Z. Rodriguez, G. Palmisano and G. Cravotto, *Synth. Commun.*, 2010, **40**, 120–128; (e) J. Xiao, Y. Chen, S. Zhu, L. Wang, L. Xu and H. Wei, *Adv. Synth. Catal.*, 2014, **356**, 1835–1845.
- 7 (a) S. Brauch, S. S. Berkel and B. Westermann, *Chem. Soc. Rev.*, 2013, **42**, 4948–4962; (b) A. Domling, W. Wang and K. Wang, *Chem. Rev.*, 2012, **112**, 3083–3135; (c) P. Slobbe, E. Ruijter and R. V. A. Orru, *Med. Chem. Commun.*, 2012, **3**, 1189–1218; (d) A. Mandal and A. T. Khan, *Org. Biomol. Chem.*, 2024, **22**, 2339–2358; (e) M. H. Sayahia, Z. Afrouzandehb and S. Bahadorikhalilic, *Process. Appl. Ceram.*, 2022, **42**, 3391–3400; (f) L. S. S. Pintoa, M. R. C. Courib and M. V. N. Souza, *Curr. Org. Synth.*, 2018, **15**, 21–37.
- 8 (a) N. N. H. Ton, H. V. Dang, N. T. S. Phan and T. T. Nguyen, *RSC Adv.*, 2019, **9**, 16215–16222; (b) M. N. Khan, S. Pal, S. Karamthulla and L. H. Choudhury, *New J. Chem.*, 2014, **38**, 4722–4729; (c) Z. Zhang, S. Zhao, Y. Wen, G. Zeng, M. Yuan and C. Huang, *Org. Biomol. Chem.*, 2025, **23**, 884–891.
- 9 (a) K. V. Sashidhara, G. R. Palnati, L. R. Singh, A. Upadhyay, S. R. Avula, A. Kumar and R. Kant, *Green Chem.*, 2015, **17**, 3766–3770; (b) T. Ataee-Kachouei, M. Nasr-Esfahani, I. Mohammadpoor-Baltork, V. Mirkhani, M. Moghadam, S. Tangestaninejad and R. Kia, *ChemistrySelect*, 2019, **4**, 2301–2306; (c) R. Singha, A. Islam and P. Ghosh, *Sci. Rep.*, 2021, **11**, 19891; (d) Z. Chen, J. Bi and W. Su, *Chin. J. Chem.*, 2013, **31**, 507–514.
- 10 S. E. Denmark and S. Venkatraman, *J. Org. Chem.*, 2006, **71**, 1668–1676.
- 11 (a) I. Bauer and H. J. Knolker, *Chem. Rev.*, 2015, **115**, 3170–3387; (b) S. Singh and S. Pal, *Chem. Commun.*, 2023, **59**, 13498–13501; (c) S. Singh, M. C. Maity and S. Pal, *J. Org. Chem.*, 2025, **90**, 3166–3171; (d) S. Singh, S. K. Mondal and S. Pal, *Org. Chem. Front.*, 2025, **12**, 5445–5452.
- 12 (a) L. Wang, M. J. Li, Q. H. Li, P. Xu, S. Q. Chen, H. Xu and Z. Zhang, *Tetrahedron Lett.*, 2025, **161**, 155569; (b) E. E. Galenko, M. A. Kryukova, M. S. Novikov and A. F. Khlebnikov, *J. Org. Chem.*, 2021, **86**, 6888–6896; (c) M. J. Li, H. J. Xiao, P. Xu, L. T. Wu, S. Q. Chen, Z. Zhang and H. Xu, *Org. Lett.*, 2024, **26**, 4189–4193; (d) S. Q. Chen, M. J. Li, P. Xu, Q. H. Li, H. Xu and Z. Zhang, *J. Org. Chem.*, 2025, **90**, 2956–2967.
- 13 (a) E. E. Galenko, V. A. Bodunov, A. V. Galenko, M. S. Novikov and A. F. Khlebnikov, *J. Org. Chem.*, 2017, **82**, 8568–8579; (b) T. A. Palazzo, D. Patra, J. S. Yang, E. Khoury, M. G. Appleton, M. J. Haddadin, D. J. Tantillo and M. J. Kurth, *Org. Lett.*, 2015, **17**, 5732–5735; (c) A. V. Galenko, F. M. Shakirova, E. E. Galenko, M. S. Novikov and A. F. Khlebnikov, *J. Org. Chem.*, 2017, **82**, 5367–5379; (d) T. O. Zanakhov, E. E. Galenko, M. S. Novikov and A. F. Khlebnikov, *Beilstein J. Org. Chem.*, 2022, **18**, 738–745.

